Vol. 19, No. 3 (2020) 1301-1313
Revista Mexicana de Ingeniería Química

Effect of processing parameters on astaxanthin nanoemulsions with stearic acid using ultrasonic emulsification

Efecto de los parámetros de procesamiento en las nanoemulsiones de astaxantina con ácido esteárico utilizando emulsificación ultrasónica

G. A. Flores-Miranda[1], J. Yáñez-Fernández[1], E. San Martin-Martínez[2]*

[1]*Departamento de Biotecnología Alimentaria, Unidad Profesional Interdisciplinaria de Biotecnología, Instituto Politécnico Nacional, Av. Acueducto S/N Col. Barrio La Laguna Ticomán, México, D.F., CP 07340, México.*
[2]*Departamento de Biomateriales, Centro de Investigación en Ciencia Aplicada y Tecnología Avanzada del Instituto Politécnico Nacional, Calzada Legaria No. 694 Col. Irrigación, México, D.F., CP 11500, México.*

Received: September 6, 2019; Accepted: January 22, 2020

Abstract

Astaxanthin is a food colorant with exceptional antioxidant activity. Here, nanoemulsions were prepared via an ultrasound emulsification method. We evaluated the effect of lipid concentration (4-7%), surfactant concentration (0.1-2.0%), and sonication time (15-30 min) on the particle size while holding astaxanthin content (0.2%) constant. To determine the particle size, transmission electron microscopy (Cryo-TEM) and dynamic light scattering were used. The antioxidant activity was studied as a function of $ABTS^{\bullet+}$ radical concentration, and a spectrophotometric method was used to study the stability of the nanoemulsions over time. The increase of the sonication time and the amount of emulsifier reduce the particle size. The best conditions to prepare stearic acid and astaxanthin nanoemulsions were 4.0% of lipid concentration and 2.0% for surfactant content employing a sonication time of 15.0 min. Having also under these conditions a lower loss of antioxidant activity and greater stability at the end of the storage period against non-emulsified astaxanthin.

Keywords: Nanoemulsion, ultrasonic emulsification, stearic acid, astaxanthin, antioxidant activity.

Resumen

La astaxantina es un colorante alimentario con una actividad antioxidante excepcional. Aquí, las nanoemulsiones se prepararon mediante un método de emulsión por ultrasonido. Evaluamos el efecto de la concentración de lípidos (4-7%), la concentración de surfactante (0.1-2.0%) y el tiempo de sonicación (15-30 min) sobre el tamaño de partícula, mientras se mantiene constante el contenido de astaxantina (0.2%). Para determinar el tamaño de las partículas se utilizó la microscopía electrónica de transmisión (Cryo-TEM) y dispersión de luz dinámica. La actividad antioxidante se estudió en función de la concentración de radicales $ABTS^{\bullet+}$, y se utilizó un método espectrofotométrico para estudiar la estabilidad de las nanoemulsiones en función del tiempo. El aumento del tiempo de sonicación y la cantidad de emulsionante reducen el tamaño de partícula. Las mejores condiciones para preparar nanoemulsiones de ácido esteárico y astaxantina fueron: 4.0% de concentración de lípidos y 2.0% para contenido de surfactante empleando un tiempo de sonicación de 15.0 min. Teniendo también en estas condiciones una menor pérdida de actividad antioxidante y una mayor estabilidad al final del período de almacenamiento frente a la astaxantina no emulsionada.

Palabras clave: Nanoemulsiones, emulsión ultrasónica, ácido esteárico, astaxantina, actividad antioxidante.

1 Introduction

Emulsions are 50 to 1000 nm dispersions and also known as microemulsions, fine dispersed emulsions, or submicron emulsions (Bhosale *et al*., 2014). Nanoemulsions consist of a lipid phase dispersed in an aqueous continuous phase with each oil droplet being surrounded by a thin interfacial layer consisting of emulsifier molecules (Acosta, 2009). Nanoemulsions are usually highly stable and do not settle by gravity because Brownian motion dominates (Ghosh *et al*., 2014). They also have good stability against droplet aggregation because the range of attractive forces between the droplets decreases with decreasing particle size (while the range of steric repulsion is less dependent) (McClements, 2004).

* *Corresponding author. E-mail*: esanmartin@ipn.mx
Tel. +52 5557296300 ext. 67769
https://doi.org/10.24275/rmiq/Alim936
issn-e: 2395-8472

These potential advantages of nanoemulsions over conventional emulsions make them attractive systems for application in food, cosmetics, and pharmaceuticals. They can act as carriers or delivery systems for lipophilic compounds such as nutraceuticals, drugs, flavors, antioxidants, and antimicrobial agents (Ghosh *et al*., 2013b; Muñoz-Correa *et al*., 2019; Kesisoglou *et al*., 2007; Sanguansri and Augustin, 2006; Weiss *et al*., 2008; Wissing *et al*., 2004).

There is an increased interest in incorporating lipid compounds into nanoemulsions. This work relies on the advantages of lipid materials in comparison to other systems, e.g. biocompatibility and biodegradation (Severino *et al*., 2011). This can also prevent the lipid autoxidation that generally involves phase transition (Basri *et al*., 2007; Hippalgaonkar *et al*., 2010). Stearic acid is an endogenous long-chain saturated fatty acid and a primary component of fats in both animal and plant sources. It provides better biocompatibility and lower toxicity than the other synthesized counterparts (Fundarò *et al*., 2000). Stearic acid has a melting point higher than body temperature (m.p. 69.6 ºC). It is biocompatible with human tissues and neutral with respect to physiological fluids. The stearic acid used here is non-toxic and is 'Generally Recognized as Safe' (GRAS) by the Food and Drug Administration (FDA) (Severino *et al*., 2011).

Various methods have been developed to prepare emulsions in the nano-size range. These are classified as either high energy or low energy approaches. Ultrasonic emulsification is a high energy method to prepare nanometer-range emulsion droplets (Ghosh *et al*., 2013a). This method is a fast and efficient technique for formulating stable nanoemulsions with very small droplet diameters and low polydispersity index (Lin and Chen, 2008). It utilizes sound waves with a frequency above 20 kHz to cause mechanical vibrations followed by the formation of acoustic cavitation. The collapse of these cavities generates powerful shocks waves that break the coarse droplets into nanoparticles (Behrend *et al*., 2000). Studies have shown that ultrasound-assisted cavitation is more competitive or even superior in terms of particle size and energy efficiency versus other typical rotational homogenizers. It can also be more economical and practical in terms of scale-up production cost, ease of maintenance, and aseptic processing (Abismaïl *et al*., 1999; Maa and Hsu, 1999; Tadros *et al*., 2004). The particle size of the nanoemulsion can be controlled by optimizing the process parameters such as lipid content, oil, emulsifier concentration, emulsification time, and energy input (Jafari *et al*., 2007; Nakabayashi *et al*., 2011).

Astaxanthin was obtained from *Haematococcus pluvialis* approved by the FDA (Food and Drug Administration) for use as a colorant in food. It is classified as GRAS (Ambati *et al*., 2014). Due to astaxanthin's exceptional antioxidant activity, it has been used as a nutraceutical (Guerin *et al*., 2003; Hussein *et al*., 2006) and against oxidative stress (Pashkow *et al*., 2008). Being a highly unsaturated molecule, it readily decomposes when exposed to heat, light, and oxygen; it also has limited solubility/dispersibility in water that hampers its applications in different areas (Higuera-Ciapara *et al*., 2006; Mezquita *et al*., 2015).

Nanotechnology can solve solubility problems of drugs and lipids via nanoencapsulation. Astaxanthin is liposoluble, and nanoencapsulation could increase its stability and preserve its antioxidant activity while evaluating the effectiveness of lipid entrapment systems (Olivarez-Romero *et al*., 2017).

Here, the effect of the factors affecting the efficiency of nanoencapsulation of astaxanthin were studied using methodology surface response (MSR). The MSR evaluated the content of lipids and surfactants as well as ultrasonication time on the physicochemical properties of the nanoemulsions. This technique has been used for different process optimization steps in food and pharmaceutical nanoemulsions (Li and Chiang, 2012; Tang *et al*., 2012; Yuan *et al*., 2008; Zainol *et al*., 2012).

2 Materials and methods

2.1 Reagents and chemicals

Stearic acid was used as the lipid core ($C_{18}H_{36}O_2$; MW = 284.5; MP = 69 °C) and was purchased from Sigma-Aldrich, USA. The food grade surfactant agent was Tween® 80 ($C_{64}H_{124}O_{26}$; Polioxietilen (20) sorbitan monooleate; non-ionic; HLB = 15.0) purchased from Sigma-Aldrich, USA. Ultrapure water from a Milli-Q system was used throughout the study.

2.2 Extraction of astaxanthin

The cysts of *Haematococcus pluvialis* algae were pretreated by mixing 5 g of algae with 1 mL of 3 M HCl and then microwaved for 1 min at 1450 W.

Next, 15 mL of ethyl acetate was added to the pretreated seaweed, and this mixture was heated in a water bath (50 °C) with constant stirring for 15 min. The sample was then centrifuged at 2,500 x g for 15 min discarding the cellular material, and the supernatant was evaporated in a rotary evaporator (Büchi Rotavapor R205, Switzerland) at 70 °C to remove the excess solvent. The extract was kept in the dark at 4 °C until use.

2.3 Nanoemulsions and solid lipid nanoparticles (SLN) of stearic acid

The stearic acid flakes were heated in a water bath 5-10 °C above its melting point (69 °C) while a mixture of deionized water/surfactant was heated to the same temperature. The molten lipid was added to the water/surfactant mixture, and the dispersion was subjected to mechanical stirring with a homogenizer Ultra-Turrax T25 (IKA, Germany) that favored the formation of the oil in water emulsion (O/W). All cases used one 10,000 rpm for 2 min.

For ultrasonic treatment, a ultrasonic processor GEX500 was used with 500 W rated power and 20 kHz frequency (Sonics & Materials Inc., USA) with a 13-mm-diameter titanium probe. This probe was introduced to the emulsion using an amplitude constant of 40%, the heat generated during the sonication was reduced with an ice bath. The nanoemulsions were analyzed in liquid and solid state after lyophilization (Labconco Freezone 4.5, USA) and called solid lipid nanoparticles (SLN).

2.4 Nanoemulsions and solid lipid nanoparticles (SLN) of astaxanthin

For the formation of oil in water nanoemulsions (O/W) of astaxanthin used two phases prepared separately. The first was astaxanthin (0.2% v/v) that was mixed with stearic acid. This mixture was heated in a water bath at 80 °C while a mixture of deionized water (Milli-Q) and Tween 80 was heated to the same temperature. Subsequently, the oily phase was added to the aqueous dispersion and then subjected to mechanical stirring in a homogenizer Ultra-Turrax T25 (IKA, Germany) at 10,000 rpm for 2 min. The ultrasonic treatment was similar to the SLN stearic acid. The heat generated during emulsification during the sonication was reduced with an ice bath. The SLNs of astaxanthin were lyophilized before subsequent characterization.

2.5 Physicochemical characterization of astaxanthin nanoemulsion

2.5.1 Particle size and polydispersity index (PDI) measurement

A Zetasizer Nano ZS (Malvern Instruments Ltd., UK) was used to determine the particle size of the emulsions via dynamic light scattering (DLS). The emulsions were analyzed 1 day after their preparation. About 1 mL of the emulsion was added to 99 mL of Milli-Q water at 25 °C to measure the particle size. The emulsion particle size was expressed as the Z-average diameter (nm). The particle size distribution curves are expressed as percent intensity vs diameter (nm). The polydispersity index (PDI) was calculated as a dimensionless unit between zero and one; a lower PDI indicates a narrower particle size distribution and vice versa.

2.5.2 Zeta (ζ) potential (ZP)

The electric charge present in the Stern layer is a useful parameter to predict the physical stability of colloidal systems and was measured using a Zetasizer Nano ZS (Malvern Instruments, UK). The samples were diluted with Milli-Q water before measurement. The samples were then injected into a folded capillary cell for ζ-potential measurement in mV. The ζ-potential values provide information on the repulsive or attractive forces between particles in the emulsion.

2.5.3 Cryo-Transmission electron microscopy (Cryo-TEM)

Cryo-TEM was made in order to confirm the particle size and characterize the shape and structure of the nanoemulsions. Samples were frozen with a Cryoplunge 3 - Cp3 (Gatan, Inc. USA). The environmental chamber was operated at 25 ºC and 73% relative humidity. Samples were diluted at the proportion of 10 μL of sample and 990 μL of Milli-Q water. A droplet of the nanoemulsion was applied to a holey carbon-coated grid. After 30 s, the suspension was blotted for 4.0 s with Whatman No. 1 filter paper using the instrument´s-blotting sensor and immediately plunged into liquid ethane just above its freezing point (-183 ºC). The vitrified samples were visualized at liquid nitrogen temperature on a JEM-2100 TEM (JEOL, USA) operating at 80 kV. To prevent recrystallization of vitreous ice, the cold stage was kept at less than -170 ºC during the observation. The micrographs were acquired a

nominal magnification of 25,000x at a defocus of -5760 nm and captured with an UltraScan XP camera.

2.5.4 *Antioxidant activity as a function of ABTS$^{\bullet+}$ radical*

This technique is based on the generation of the ABTS$^{\bullet+}$ radical cation (blue-green chromophore) via the oxidation of acid 2,2'-azino-bis (3-ethylbenzothiazoline-6-sulfonic) (ABTS) with potassium persulfate ($K_2S_2O_8$). The radical ABTS$^{\bullet+}$ was generated by the preparing of a solution of ABTS$^{\bullet+}$ 7 mM with 2.45 mM of $K_2S_2O_8$; this was incubated at room temperature in the dark conditions for a period of 16 h (Wojdyło *et al*., 2007).

The color is blue-green and remains stable for 48 h. Once formed, the radical ABTS$^{\bullet+}$ was diluted with ethanol to obtain an absorbance value between 0.7 ± 0.1 at a wavelength of 734 nm. Of the reactive set, 2 mL was taken for each test, and 20 uL of test sample was added to each. The absorbance at 1 minutes or 6 minutes of reaction was read at a wavelength of 734 nm in a spectrophotometer Lambda XLS (Perkin Elmer, USA) using ethanol as the blank. Assays were performed in triplicate. The free radical scavenging capacity was determined by equation 1:

$$AA(\%) = \frac{Abs_{ABTS} - Abs\ sample\ 6\ min}{Abs_{ABTS}} \times 100 \quad (1)$$

2.5.5 *Evaluation of stability of nanoemulsions to different storage times*

The stability of the astaxanthin nanoemulsions was evaluated by placing 30 mL of each formulation in 50-mL Falcon tubes and stored at 4 °C for 28 days. The residual concentration of pigment and loss of antioxidant activity was evaluated every 7 days. The extraction of the pigment from the encapsulating material was evaluated using spectrophotometry.

2.5.6 *Spectrophotometric quantification of astaxanthin in nanoemulsions*

The astaxanthin concentration in the emulsions was determined according to (Bustos-Garza *et al*., 2013) with minor modifications. The pigment extraction was performed by placing 1 mL of emulsion, 1 mL of methanol, and 2.5 mL of ethyl acetate in a test tube, and stirring vigorously on a vortex at maximum speed for 5 min followed by separating the pigment of the coating material. The ethyl acetate was collected for analysis. For lyophilization, 250 mg powder, 1 mL of 25% brine, 1 mL of methanol, and 2.5 mL of ethyl acetate were vortexed and ethyl acetate was collected. The astaxanthin concentration was obtained by reference to a standard curve of astaxanthin (98% Sigma, Switzerland) under the same conditions. The absorbance (Lambda XLS, Perkin Elmer, USA) at 476 nm was measured to quantify the residual concentration of the cargo; the antioxidant activity was performed as described above.

2.5.7 *Statistical analysis: Central composite design*

A central composite design (CCD) of the response surface methodology (RSM), was used to determine the effect of independent variables: stearic acid concentration (4.0-7.0%, X_1), Tween 80 concentration (0.1-2.0%, X_2), and sonication time (15-30 min, X_3) as well as their interactions on the particle size (Y). Thus, a total of 20 experimental runs were done as generated via Design-Expert version 7.1.6 software (Stat-Ease Inc., Minneapolis, USA) with three independent variables at five levels for each variable that involved 8 factorial points, 6 axial points, and 6 replicates of center points. The experiments were carried out at random to minimize the effects of unexplained variability in the actual responses due to extraneous factors. The independent variables, their levels, and the CCD scheme are listed in Table 1.

Data on the response variables are the means for each sample. Different superscript letters in the same column indicate statistical significance ($p < 0.05$) according to the Duncan least significant difference test. Statistical analysis was conducted using SAS (Statistical Analysis System Version 9.0); one-way variance analysis (ANOVA) was applied to determine the significance of the differences between assays.

3 Results and discussion

3.1 *Particle size of the stearic acid nanoemulsions*

The particle size values of the stearic acid nanoemulsions obtained from all the experiments via dynamic light scattering (DLS) are given in Table 1. The experimental data were used to calculate the coefficients of the polynomial equation (Eq. 2), which were used to predict the particle size. ANOVA showed that the polynomial equation model was

significant (P= 0.0096) and adequately represented the experimental data with a coefficient of determination (R^2) of 0.82.

$$Y = -50.11 + 59.89X_1 - 1220.10X_2 + 34.14X_3 + 219.23X_1X_2 - 6.26X_1X_3 - 7.48X_2X_3 + 570.04X_2^2 + 0.36X_3^2 - 93.69X_1X_2^2 \quad (2)$$

here, Y is the particle size (nm), X_1, and X_2 are stearic acid and Tween 80 concentration respectively, and X_3 is the sonication time.

To better understand the interaction effects of variables on particle size, the figures of response surface were plotted against two independent variables (stearic acid and Tween 80 concentration); the other variables (sonication time) were kept at its lower (-1), central (0) and higher (+1) levels, respectively. Fig. 1A shows that increasing the surfactant content decreases the particle size of the nanoemulsions with higher concentrations for 7.0% stearic acid. In fact, Mehmood (2015) pointed out that particle size decreased with increasing surfactant concentrations due to their effects on the interfacial tension of oil-water mixture.

Li and Chang (2012) stated that an increase of surfactant content between 1-7% (w/w) results in a smaller particle size and could be explained by the role of the surfactant in reducing the surface tension of the nanoemulsions and preventing their aggregation. Fig. 1A shows that a lower concentration of stearic acid (<6%) and Tween 80 (<than 1.5%) can lead to a smaller size of nanoemulsions; however, an excessive surfactant concentration might have the opposite effect. This would result in the coalescence of the emulsion droplets.

When the sonication time is increased to 22.5 min (Fig. 1B), the size of nanoemulsions is very similar to those seen in Fig. 1A (15 min sonication). Smaller nanoemulsions (~10 nm) are obtained with 7.5% stearic acid and 2.5% Tween 80. Ultrasonication time is an important parameter related to the thermodynamic equilibrium in an o/w nanoemulsion system and affects the rate of adsorption of surfactants to the droplet surface and the particle size distribution.

As sonication time increases to 30 min (Fig. 1C), smaller particles (~5 nm) are obtained at higher concentrations of stearic acid (> 7%) and Tween 80 (> 2.1%). Fig. 1C shows that there was a significant increase in the size of nanoemulsions at lower concentrations of stearic acid and Tween 80. In most cases, increasing the ultrasonic amplitude or irradiation time generally resulted in a reduction in the average particle size. This behavior has been described in the literature previously (Fathi *et al*., 2012; Kentish *et al*., 2008; Li and Chiang, 2012; Rebolleda *et al*., 2015; Tang *et al*., 2012).

The larger size of the nanoemulsions might be attributed to the effect of over-processing the emulsion, which lead to the coalescence of droplets (Ghosh *et al*., 2013a). Another possible explanation is due to a higher ultrasonic irradiation time, intense local turbulence, and shear flow field. These are generated in the vicinity of the microtip probe, and this larger turbulent force promotes a higher rate of collision between droplets.

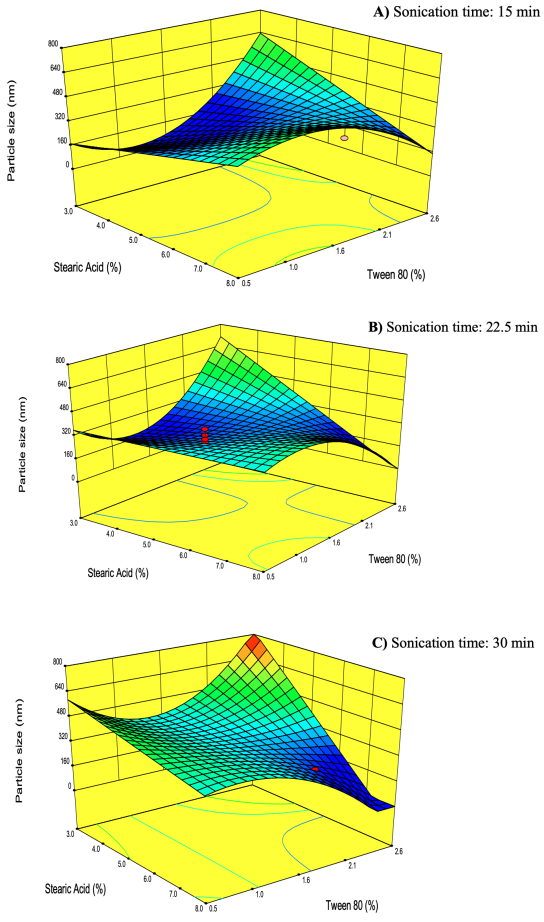

Fig. 1. Three-dimensional (3-D) response surface plots of the particle size of the nanoemulsions as a function of the concentration of stearic acid and Tween 80 at different sonication times A) 15 min, B) 22.5 min and C) 30.0 min.

Therefore, the neighboring droplets adjacent to the region of acoustic radiation forces would tend to coalesce and form larger emulsion droplets thereby resulting in an increased particle size (Tang *et al*., 2012).

3.2 Polydispersity index (PDI)

The PDI is a dimensionless measure of the width of particle size distribution and characterizes the disperse systems with respect to deviation from the average size ranging from 0 to 1. A small value of PDI indicates a monodispersed population while a large PDI indicates a broader distribution of particle size, which should be low for the long-term stability of the nanodispersions (Tang *et al*., 2012). The PDI values are 0.125 to 0.750. Here, samples with PDI values greater than 0.5 indicate a very broad distribution (Table 1).

Table 1 shows the variation in PDI of stearic acid nanoemulsions as a function of stearic acid concentration and sonication time. The last one was the principal factor that affected this response ($P< 0.05$). Low PDI values were seen at low sonication times (Table 1), and increasing the sonication time would lead to an increase in PDI because it promotes a high coalescence rate resulting in a large particle size. This led to a high polydispersity index. The PDI results are related to the size of the nanoemulsions, which means that higher concentrations of stearic acid (> 7.0%), 0.1% Tween 80, and 15 min of sonication lead to smaller particles and lower PDI values. Sonication time increments of 30 min for the same synthesis conditions lead to ~ 450 nm nanoemulsions with a higher PDI.

The concentration of stearic acid also affects the distribution or the value of PDI. The lower concentration (4.0%) of particles have a bimodal distribution with most at 315 nm and a minor peak at 1500 nm; these used 15 min of sonication time. There were 775 nm and 1500 nm nanoparticles at greater sonication times (30 min) and the same concentration of steric acid (4.0%). Thus, 7.0% steric acid and 15 min of sonication time gave stable and homogeneous nanoemulsions.

Table 1. CCD scheme: independent (X_i) and response variable (Y_j).

	Independent Variables			Particle size (nm)	Polydispersity index (PDI)
Run	X_1	X_2	X_3	Experimental (Yj)	
F1	7.00	0.10	15.00	356.30 ± 1.35 ^{e}	0.125 ± 0.04 ^{h}
F2	4.00	2.00	15.00	270.10 ± 5.21 ^{fgh}	0.131 ± 0.02 ^{h}
F3	7.00	0.10	30.00	372.47 ± 4.02 ^{de}	0.195 ± 0.03 ^{gh}
F4	2.98	1.05	22.50	238.13 ± 45.04 ^{h}	0.603 ± 0.05 ^{bc}
F5	4.00	2.00	30.00	354.90 ± 17.25 ^{e}	0.678 ± 0.08 ^{ab}
F6	5.50	1.05	35.11	497.53 ± 85.88 ^{bc}	0.597 ± 0.02 ^{bc}
F7	8.02	1.05	22.50	469.73 ± 54.59 ^{c}	0.581 ± 0.12 ^{bc}
F8	7.00	2.00	15.00	277.07 ± 37.36 ^{fgh}	0.502 ± 0.05 ^{cd}
F9	5.50	1.05	9.89	325.27 ± 4.51 ^{ef}	0.297 ± 0.03 ^{fg}
F10	4.00	0.10	30.00	775.47 ± 18.97 ^{a}	0.441 ± 0.06 ^{de}
F11	5.50	0.55	22.50	555.30 ± 75.39 ^{b}	0.750 ± 0.06 ^{a}
F12	7.00	2.00	30.00	244.23 ± 4.36 ^{gh}	0.366 ± 0.02 ^{ef}
F13	4.00	0.10	15.00	313.37 ± 32.02 ^{efg}	0.365 ± 0.02 ^{ef}
F14	5.50	2.65	22.50	432.87 ± 17.29 ^{cd}	0.440 ± 0.07 ^{de}
*F15	5.50	1.05	22.50	321.31 ± 52.46 ^{ef}	0.429 ± 0.15 ^{de}

X_1: stearic acid concentration (% w/w), X_2: Tween 80 concentration (% w/w), X_3: sonication time (min). *Average of six replicates at the center point.

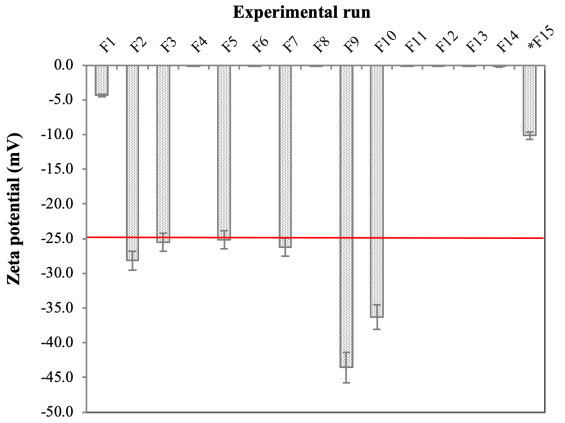

Fig. 2. Effect of processing parameters of ultrasound emulsification on the ZP of stearic acid nanoemulsions. The data represent the means ± deviation standard. *Average of six replicates at the center point.

3.3 *Zeta potential (ZP) of the stearic acid nanoemulsions*

Droplets with electrical charge above +30 mV or below -30 mV are considered to be stable within the nanoemulsion system (Heurtault *et al*., 2003). This arbitrary value separates low charged surfaces from highly charged surfaces.

Determining the zeta potential may provide information on system stability because the particles surface charge can prolong the stability of formulations by electrostatic repulsion this prevents destabilization phenomena such as droplet coalescence and Ostwald ripening (Lim *et al*., 2011; Flores-Hernández *et al*., 2019). The ZP values of stearic acid nanoemulsions are shown in Fig. 2 and ranged between 0.01 to -43.5 mV. In general, the electrical charge of droplets is governed by the charge in surfactants adsorbed around the oil droplets this can be anionic, cationic or non-ionic nature. The nanoemulsions prepared here contained a non-ionic surfactant (Tween 80); hence, the absolute magnitude of droplet charge is very low in some formulations. In this case, system stability occurs mainly by steric stabilization rather than electrostatic stabilization, and F9 and F10 formulation nanoemulsions were very stable (Fig 2). The ZP is influenced by many factors such as the source of particles, surfactants, electrolyte concentrations (ionic strength), particle morphology, size, pH of the solution, and state of hydration (Simunkova *et al*., 2009).

The values (-25 mV) can also be considered stable for the purposes of repulsion. This charge will minimize aggregation. F2 samples (Table 1) would be stable for its size (270.10 nm) and PDI (0.131).

3.4 *Cryo-Transmission electron microscopy (Cryo-TEM)*

Cryo-TEM studies were performed to better understand the microstructure of the nanoemulsions. The microscopic investigations confirmed the DLS data. DLS alone has certain limitations for particle size analysis of nanoemulsions; thus, an additional technique such as cryo-TEM is strongly recommended (Klang *et al*., 2012). Fig. 4a shows that the nanoemulsion droplets of all formulations are spherical and homogeneous with a size in the nanometer range (<700 nm). In particular, the particle size of the F5 formulation was measured, and this observation reveals spherical shapes with a particle size of 362.7 nm; the mean particle size was determined by DLS (354.9 ± 17.2 nm), which is in good agreement with the microscopically-observed particle sizes.

3.5 *Physicochemical characterization of nanoemulsion of astaxanthin*

3.5.1 *Particle size, PDI, and ZP of astaxanthin nanoemulsions*

F1, F4, F5, F16, and F18 conditions were used for nanoencapsulation of astaxanthin. To observe the effect of ascending concentration of steric acid on the synthesis of nanoemulsions (F4, 2.98% w/w), (F5, 4.00% w/w), (F16 and F18, 5.50% w/w), (F1, 7.00% w/w) on the size of nanoemulsions, PDI and ZP values. These were prepared according to the conditions shown in Table 1, and the astaxanthin content (0.2%) remained constant for the five formulations.

Table 2 shows the particle size of the nanoemulsions of astaxanthin from 225.70 to 341.83 nm. Statistically significant differences ($p < 0.05$) were observed. An increase in the surfactant concentration resulted in a decrease in particle size while long sonication times generated larger nanoemulsions.

Nanoemulsions were obtained with different particle sizes depending on the method and the polymeric constituents. For example, Anarjan *et al*. (2013) reported smaller particle sizes for nanoemulsions using astaxanthin, gum arabic, Tween 20, and sodium caseinate.

Table 2. Particle size, PDI, and ZP of astaxanthin nanoemulsions.

Formulation	Particle size (nm)	PDI	ZP (mV)
F1	225.70 ± 2.16^{d}	0.251 ± 0.01b	-0.025 ± 0.06^{a}
F4	277.13 ± 3.31^{c}	0.340 ± 0.04a	-30.60 ± 1.11^{c}
F5	276.17 ± 9.61^{c}	0.223 ± 0.01b	-26.60 ± 0.40^{b}
F16	303.57 ± 13.05^{b}	0.335 ± 0.02a	-26.66 ± 0.72^{b}
F18	341.83 ± 12.61^{a}	0.376 ± 0.07a	$- 30.76 \pm 1.17^{c}$

The experimental values are mean of each sample (n = 3). Means with different letter in the same column indicate significant differences ($p < 0.05$) according to Duncan's test.

This led to emulsification-evaporation with sizes between 90.29 - 139.10 nm. Anarjan *et al*. (2014) obtained particles between 122-209 nm when prepared with gelatin and acacia via high-pressure homogenization.

The PDI for the astaxanthin nanoemulsions are 0.223-0.376 (Table 2) indicating monodisperse systems. The results showed that the concentration of Tween had a significant effect ($p < 0.05$) on the PDI, which showed a greater effect. This effect was attributed to the nature of the surfactant, its rate of diffusion, and the effect of surface that prevents aggregation between the nanoemulsions. This influences the particle size reduction and produces more homogeneous systems.

The ZP values are shown in Table 2 and range from -0.025 to -30.76 mV. In this case, the formulations were highly stable systems except for F1. Lower values (-15.30 mV) were reported by Anarjan *et al*. (2014) for astaxanthin nanodispersions produced via high-pressure homogenization. Both systems have a negative surface charge. Many authors mention that this behavior may be associated with the OH groups of astaxanthin (Anarjan *et al*., 2012; Yin *et al*., 2009). Thus, F5 was found to be best based on particle size, PDI, and ZP (Table 2).

3.5.2 Evaluation of the degradation of astaxanthin pigment in nanoemulsions

The effect of storage conditions on the concentration of astaxanthin in the nanoemulsions was monitored by a spectrophotometric method as described in the methodology. The pigment concentration gradually decreased during the storage period. The residual concentration of pigment in the control (astaxanthin, not nanoemulsified) fell from 428.72 to 132.97 mg/mL and exhibited degradation of 68.99% at the end of the storage period of 28 days. F5, F16m and F18 nanoemulsions had a degradation percentage that ranged from 27 to 31%. It was less than non-nanoemulsified astaxanthin. Formulations with ZP values between -30.76 mV and -26.6 mV (Table 2) had less degradation. The stability of astaxanthin is improved with the nanoemulsions.

According to Tamjidi *et al*. (2014), the degradation of astaxanthin can be attributed to the effect of different process parameters such as temperature increase and the incorporation of oxygen due to cavitation during sonic emulsification. In spite of these limitations, pigment degradation was lower in the nanoemulsions versus non-nanoemulsified astaxanthin. The storage conditions of the nanoemulsions also visibly affected the concentration of astaxanthin after 28 days due to the effect of light and oxygen on the bioactive component (Boon *et al*., 2010).

3.5.3 Evaluation of the antioxidant activity of astaxanthin nanoemulsions

Fig. 3 shows the percent inhibition for each formulation prepared and evaluated over a 28-day period at 4 °C is shown. This percentage represents the amount of radical $ABTS^{\bullet+}$ that produces a color change from blue to colorless when in contact with a substance having antioxidant activity. This change was measured by spectrophotometric method at 734 nm.

The antioxidant activity of astaxanthin nanoemulsions was influenced by storage conditions. Fig. 3 shows that both the control (astaxanthin not nanoemulsified) and the formulations had a decrease in percent of antioxidant activity after 28 days storage. The unencapsualted astaxanthin decreased from 62.54 to 24.69% (60.52% loss). Nanoemulsions of astaxanthin had activity losses less than 50% (between 27.2 and 40.19%). Similar results were seen by Taksima *et al*. (2015).

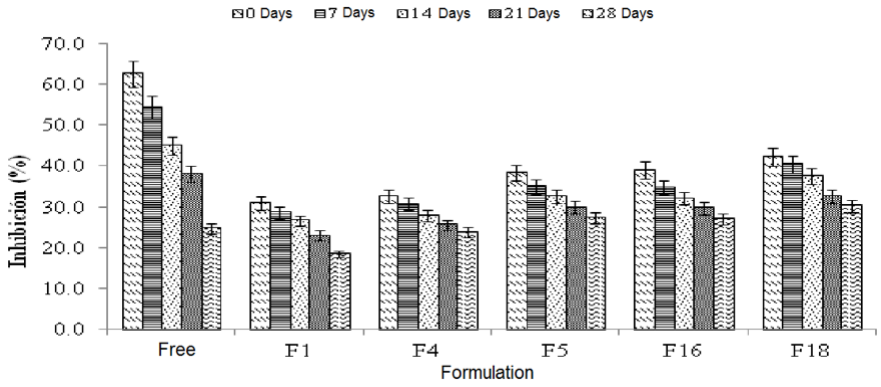

Fig. 3. Effect of storage time on the antioxidant activity of astaxanthin nanoemulsions.

Their reduction was above 80% for control and smaller reductions of 50% for astaxanthin encapsulated in alginate-chitosan beads sample. Thus, the entrapment system protects the active compound. The F4, F5, F16 and F18 formulations best protected astaxanthin. These formulations showed the highest stability via ZP. These results confirmed that the encapsulation of the astaxanthin in nanoemulsions allowed the conservation of antioxidant activity mediated by donating electrons to neutralize free radicals (Kidd, 2011).

3.5.4 TEM at cryogenic temperature (Cryo-TEM) of nanoemulsions of astaxanthin

Cryo-analysis was performed with TEM to determine the shape and size of the droplets present in the nanoemulsions of astaxanthin. Microscopic analysis was used to confirm the values of particle size by DLS technique (Schwarz *et al*., 2012) and showed that DLS has limitations for analyzing particle size; thus, complementary techniques like Cryo-TEM is widely recommended (Klang *et al*., 2012). Fig. 4b revealed spherical and homogeneous forms with a particle size of 195 nm for F5. This value was close to that obtained by DLS (276 nm). This morphology was similar to that reported previously (Affandi *et al*., 2011) showing well-defined spherical shapes of the droplets in the nanoemulsions of astaxanthin. The micrographs show dark areas within the nanoparticles. Tachaprutinun *et al*. (2009) reported that these dark zones in the core nanoparticles are attributed to the presence of astaxanthin in the polymer matrix of encapsulation.

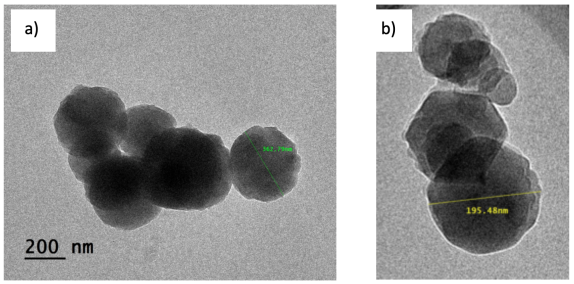

Fig. 4. Images of nanoemulsions by Cryo-TEM corresponding to the formulation F5 containing 4% stearic acid, 2.0% Tween 80 and 30 min of sonication time a) without astaxanthin, b) containing 0.20% astaxanthin.

Conclusions

The time of sonication followed by amount of emulsifier significantly affect ($p < 0.05$) the size of the nanoemulsions. The ideal values were 4.0% of stearic acid, 2.0% for Tween 80, and 15.0 min of sonication time. This led to 198.46 nm particles. Cryo-TEM confirmed the mean particle sizes to be 360 nm as seen in DLS. The nanoemulsions of astaxanthin from F5 conditions (container containing 0.20% astaxanthin, 5% stearic acid, 2.0% Tween 80, and 30 min of sonication time) are stable (276 nm) with reduced antioxidant activity losses. These results underscore the potential capability of this ultrasonic technique for producing nano-scale emulsions. It is a relatively simple, effective, and powerful emulsification method for producing stearic acid nanoemulsions. It can incorporate astaxanthin with reasonable stability.

Acknowledgements

Grisel Adriana Flores-Miranda acknowledges to CONACyT-México for a scholarship for Ph.D. studies. We thank Dr. Raul Borja-Urby at CNMN-IPN for his valuable assistance with the Cryo-TEM.

References

Acosta E. (2009). Bioavailability of nanoparticles in nutrient and nutraceutical delivery. *Current Opinion in Colloid & Interface Science 14*, 3-15. https://doi.org/10.1016/j.cocis.2008.01.002

Abismaïl, B., Canselier, J. P., Wilhelm, A. M., Delmas, H., and Gourdon, C. (1999). Emulsification by ultrasound: drop size distribution and stability. *Ultrasonics Sonochemistry 6*, 75-83.

Affandi, M. M., Julianto, T., and Majeed, A. (2011). Development and stability evaluation of astaxanthin nanoemulsion. *Asian Journal of Pharmaceutical and Clinical Research 4*, 143-148.

Ambati, R. R., Siew Moi, P., Ravi, S., and Aswathanarayana, R. G. (2014). Astaxanthin: sources, extraction, stability, biological activities and its commercial applications−A review. *Marine Drugs 12*, 128-152.

Anarjan, N., Nehdi, I., Sbihi, H., Al-Resayes, S., Malmiri, H., and Tan, C. (2014). Preparation of astaxanthin nanodispersions using gelatin-based stabilizer systems. *Molecules 19*, 14257.

Anarjan, N., Nehdi, I. A., and Tan, C. P. (2013). Influence of astaxanthin, emulsifier and organic phase concentration on physicochemical properties of astaxanthin nanodispersions. *Chemistry Central Journal 7*, 127-127.

Anarjan, N., Tan, C. P., Nehdi, I. A., and Ling, T. C. (2012). Colloidal astaxanthin: Preparation, characterisation and bioavailability evaluation. *Food Chemistry 135*, 1303-1309.

Basri, M., Rahman, R. N., Ebrahimpour, A., Salleh, A. B., Gunawan, E. R., and Rahman, M. B. (2007). Comparison of estimation capabilities of response surface methodology (RSM) with artificial neural network (ANN) in lipase-catalyzed synthesis of palm-based wax ester. *BMC Biotechnology 7*, 53.

Behrend, O., Ax, K., and Schubert, H. (2000). Influence of continuous phase viscosity on emulsification by ultrasound. *Ultrasonics Sonochemistry 7*, 77-85.

Bhosale, R. R., Osmani, R. A., Ghodake, P. P., Shaikh, S. M., and Chavan, S. R. (2014). Nanoemulsion: a review on novel profusion in advanced drug delivery. *Indian Journal of Pharmaceutical and Biological Research 2*, 122.

Boon, C. S., McClements, D. J., Weiss, J., and Decker, E. A. (2010). Factors influencing the chemical stability of carotenoids in foods. *Critical Reviews in Food Science and Nutrition 50*, 515-532.

Bustos-Garza, C., Yáñez-Fernández, J., and Barragán-Huerta, B. E. (2013). Thermal and pH stability of spray-dried encapsulated astaxanthin oleoresin from *Haematococcus pluvialis* using several encapsulation wall materials. *Food Research International 54*, 641-649.

Fathi, M., Mozafari, M. R., and Mohebbi, M. (2012). Nanoencapsulation of food ingredients using lipid based delivery systems. *Trends in Food Science & Technology 23*, 13-27.

Flores-Hernández, E., Lira-Saldívar, R., Acosta-Ortiz, R., Méndez-Arguello, B., García-López, J., Díaz-Barriga-Castro, E., González-Torres, A., & García-Carrillo, M. (2019). Synthesis and characterization of calcium phosphate nanoparticles and effect of the agitation type on particles morphology. *Revista Mexicana de Ingeniería Química 19*, 285-298.

Fundarò, A., Cavalli, R., Bargoni, A., Vighetto, D., Zara, G. P., and Gasco, M. R. (2000). Non-stealth and stealth solid lipid nanoparticles (SLN) carrying doxorubicin: pharmacokinetics and tissue distribution after i.v. administration to rats. *Pharmacological Research 42*, 337-343.

Ghosh, V., Mukherjee, A., and Chandrasekaran, N. (2013a). Influence of process parameters on droplet size of nanoemulsion formulated by ultrasound cavitation. *Journal of Bionanoscience 7*, 580-584.

Ghosh, V., Mukherjee, A., and Chandrasekaran, N. (2013b). Ultrasonic emulsification of food-grade nanoemulsion formulation and evaluation of its bactericidal activity. *Ultrasonics Sonochemistry 20*, 338-344.

Ghosh, V., Mukherjee, A., and Chandrasekaran, N. (2014). Optimization of process parameters to formulate nanoemulsion by spontaneous emulsification: evaluation of larvicidal activity against *Culex quinquefasciatus* larva. *BioNanoScience 4*, 157-165.

Guerin, M., Huntley, M. E., and Olaizola, M. (2003). Haematococcus astaxanthin: applications for human health and nutrition. *Trends in Biotechnology 21*, 210-216.

Heurtault, B., Saulnier, P., Pech, B., Proust, J.-E., and Benoit, J.-P. (2003). Physico-chemical stability of colloidal lipid particles. *Biomaterials 24*, 4283-4300.

Higuera-Ciapara, I., Félix-Valenzuela, L., and Goycoolea, F. M. (2006). Astaxanthin: a review of its chemistry and applications. *Critical Reviews in Food Science and Nutrition 46*, 185-196.

Hippalgaonkar, K., Majumdar, S., and Kansara, V. (2010). Injectable lipid emulsions−advancements, opportunities and challenges. *AAPS PharmSciTech 11*, 1526-1540.

Hussein, G., Sankawa, U., Goto, H., Matsumoto, K., and Watanabe, H. (2006). Astaxanthin, a carotenoid with potential in human health and nutrition. *Journal of Natural Products 69*, 443-449.

Jafari, S. M., He, Y., and Bhandari, B. (2007). Production of sub-micron emulsions by ultrasound and microfluidization techniques. *Journal of Food Engineering 82*, 478-488.

Kentish, S., Wooster, T. J., Ashokkumar, M., Balachandran, S., Mawson, R., and Simons, L. (2008). The use of ultrasonics for nanoemulsion preparation. *Innovative Food Science & Emerging Technologies 9*, 170-175.

Kesisoglou, F., Panmai, S., and Wu, Y. (2007). Application of nanoparticles in oral delivery of immediate release formulations. *Current Nanoscience 3*, 183-190.

Kidd, P. (2011). Astaxanthin, cell membrane nutrient with diverse clinical benefits and anti-aging potential. *Alternative Medicine Review 16*, 355-64.

Klang, V., Matsko, N. B., Valenta, C., and Hofer, F. (2012). Electron microscopy of nanoemulsions: An essential tool for characterisation and stability assessment. *Micron 43*, 85-103.

Li, P.-H., and Chiang, B.-H. (2012). Process optimization and stability of d-limonene-in-water nanoemulsions prepared by ultrasonic emulsification using response surface methodology. *Ultrasonics Sonochemistry 19*, 192-197.

Lim, S. S., Baik, M. Y., Decker, E. A., Henson, L., Michael Popplewell, L., McClements, D. J., and Choi, S. J. (2011). Stabilization of orange oil-in-water emulsions: A new role for ester gum as an Ostwald ripening inhibitor. *Food Chemistry 128*, 1023-1028.

Lin, C.-Y., and Chen, L.-W. (2008). Comparison of fuel properties and emission characteristics of two- and three-phase emulsions prepared by ultrasonically vibrating and mechanically homogenizing emulsification methods. *Fuel 87*, 2154-2161.

Maa, Y.-F., and Hsu, C. C. (1999). Performance of sonication and microfluidization for liquid-liquid emulsification. *Pharmaceutical Development and Technology 4*, 233-240.

McClements, D. J. (2004). *Food Emulsions: Principles, Practices, and Techniques*. CRC press.

Mehmood, T. (2015). Optimization of the canola oil based vitamin E nanoemulsions stabilized by food grade mixed surfactants using response surface methodology. *Food Chemistry 183*, 1-7.

Mezquita, P. C., Huerta, B. E. B., Ramírez, J. C. P., and Hinojosa, C. P. O. (2015). Milks pigmentation with astaxanthin and determination of colour stability during short period cold storage. *Journal of Food Science and Technology 52*, 1634-1641.

Muñoz-Correa, M., Bravo-Alfaro, D., García, H., & Garcia-Varela, R. (2019). Development of a self-nanoemulsifying drug delivery system (SNEDDS) from an insulin complex with modified phosphatidylcholine and mucoadhesive polysaccharide coating as a potential none-invasive treatment for diabetes. *Revista Mexicana de Ingeniería Química 19*, 49-58.

Nakabayashi, K., Amemiya, F., Fuchigami, T., Machida, K., Takeda, S., Tamamitsu, K., and Atobe, M. (2011). Highly clear and transparent nanoemulsion preparation under surfactant-free conditions using tandem acoustic emulsification. *Chemical Communications 47*, 5765-5767.

Olivarez-Romero, R., Faustino-Vega, A., Miranda-Calderon, J., González-Vázquez, R., & Azaola-Espinosa, A. (2018). Microencapsulation of *Lactobacillus acidophilus* la-5 increases relative survival under simulated gastrointestinal tract stress. *Revista Mexicana de Ingeniería Química 17*, 641-650.

Pashkow, F. J., Watumull, D. G., and Campbell, C. L. (2008). Astaxanthin: a novel potential treatment for oxidative stress and inflammation in cardiovascular disease. *The American Journal of Cardiology 101*, S58-S68.

Rebolleda, S., Sanz, M. T., Benito, J. M., Beltrán, S., Escudero, I., and González San-José, M. L. (2015). Formulation and characterisation of wheat bran oil-in-water nanoemulsions. *Food Chemistry 167*, 16-23.

Sanguansri, P., and Augustin, M. A. (2006). Nanoscale materials development-a food industry perspective. *Trends in Food Science & Technology 17*, 547-556.

Schwarz, J. C., Klang, V., Karall, S., Mahrhauser, D., Resch, G. P., and Valenta, C. (2012). Optimisation of multiple W/O/W nanoemulsions for dermal delivery of aciclovir. *International Journal of Pharmaceutics 435*, 69-75.

Severino, P., Pinho, S. C., Souto, E. B., and Santana, M. H. (2011). Polymorphism, crystallinity and hydrophilic-lipophilic balance of stearic acid and stearic acid-capric/caprylic triglyceride matrices for production of stable nanoparticles. *Colloids and Surfaces B: Biointerfaces 86*, 125-130.

Simunkova, H., Pessenda-Garcia, P., Wosik, J., Angerer, P., Kronberger, H., and Nauer, G. E. (2009). The fundamentals of nano- and submicro-scaled ceramic particles incorporation into electrodeposited nickel layers: Zeta potential measurements. *Surface and Coatings Technology 203*, 1806-1814.

Tachaprutinun, A., Udomsup, T., Luadthong, C., and Wanichwecharungruang, S. (2009). Preventing the thermal degradation of astaxanthin through nanoencapsulation. *International Journal of Pharmaceutics 374*, 119-124.

Tadros, T., Izquierdo, P., Esquena, J., and Solans, C. (2004). Formation and stability of nano-emulsions. *Advances in colloid and Interface Science 108*, 303-318.

Taksima, T., Limpawattana, M., and Klaypradit, W. (2015). Astaxanthin encapsulated in beads using ultrasonic atomizer and application in yogurt as evaluated by consumer sensory profile. *LWT - Food Science and Technology 62*, 431-437.

Tamjidi, F., Shahedi, M., Varshosaz, J., and Nasirpour, A. (2014). Design and characterization of astaxanthin-loaded nanostructured lipid carriers. *Innovative Food Science & Emerging Technologies 26*, 366-374.

Tang, S. Y., Manickam, S., Wei, T. K., and Nashiru, B. (2012). Formulation development and optimization of a novel Cremophore EL-based nanoemulsion using ultrasound cavitation. *Ultrasonics Sonochemistry 19*, 330-345.

Weiss, J., Decker, E. A., McClements, D. J., Kristbergsson, K., Helgason, T., and Awad, T. (2008). Solid lipid nanoparticles as delivery systems for bioactive food components. *Food Biophysics 3*, 146-154.

Wissing, S. A., Kayser, O., and Müller, R. H. (2004). Solid lipid nanoparticles for parenteral drug delivery. *Advanced Drug Delivery Reviews 56*, 1257-1272.

Wojdyło, A., Oszmiański, J., and Czemerys, R. (2007). Antioxidant activity and phenolic compounds in 32 selected herbs. *Food Chemistry 105*, 940-949.

Yin, L.-J., Chu, B.-S., Kobayashi, I., and Nakajima, M. (2009). Performance of selected emulsifiers and their combinations in the preparation of β-carotene nanodispersions. *Food Hydrocolloids 23*, 1617-1622.

Yuan, Y., Gao, Y., Mao, L., and Zhao, J. (2008). Optimisation of conditions for the preparation of β-carotene nanoemulsions using response surface methodology. *Food Chemistry 107*, 1300-1306.

Zainol, S., Basri, M., Basri, H. B., Shamsuddin, A. F., Abdul-Gani, S. S., Karjiban, R. A., and Abdul-Malek, E. (2012). Formulation optimization of a palm-based nanoemulsion system containing levodopa. *International Journal of Molecular Sciences 13*, 13049-13064.